ORGANOMETALLICS

pubs.acs.org/Organometallics

Article

Germanium-Functionalized Tri- and Tetraphosphido Cobalt Complexes

Published as part of Organometallics special issue "Organometallic Chemistry Beyond the Transition Metals: Fundamentals and Applications of the P-Block".

Karolina Trabitsch, Sebastian Hauer, Gábor Balázs, Jan J. Weigand, and Robert Wolf*

Cite This: *Organometallics* 2025, 44, 1721−1727

Read Online

ACCESS | Metrics & More | Article Recommendations | Supporting Information

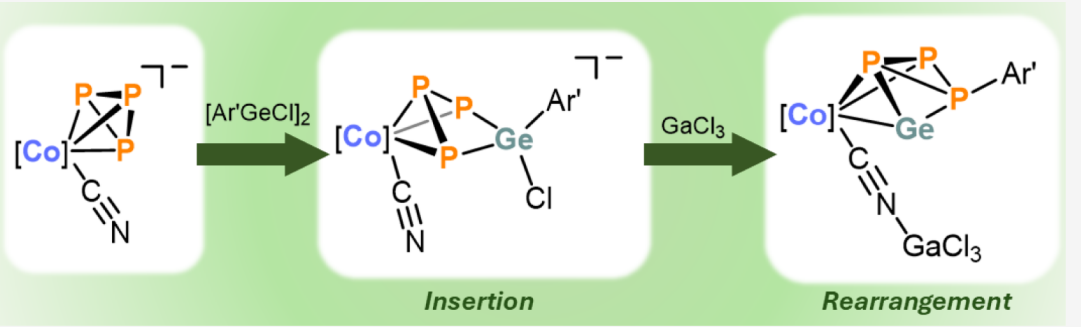

ABSTRACT: We report the synthesis of germanium-containing polyphosphorus ligands in transition metal complexes through the insertion of an Ar′GeCl unit into a P−P bond of polyphosphorus ligands (Ar′ = 2,6-(2,6-*i*Pr$_2$C$_6$H$_3$)$_2$-C$_6$H$_3$). Germatetraphosphido complexes [(L)Co(η^4-P$_4$GeAr′)] (**1a**: L = PHDI; **1b**: L = Ar*BIAN; PHDI = bis(2,6-diisopropylphenyl)phenanthrene-9,10-diimine, Ar*BIAN = 1,2-bis(arylimino)acenaphthene, aryl = 2,6-dibenzhydryl-4-isopropylphenyl) were obtained by treatment of the anionic *cyclo*-P$_4$ complexes [K(18c-6)][(L)Co(η^4-P$_4$)] with [Ar′GeCl]$_2$. Similar reactions of the *cyclo*-P$_3$ complexes [cat][(L)Co(CN)(η^3-P$_3$)] ([cat]$^+$ = [*n*Bu$_4$N]$^+$ or [K(18c-6)]$^+$) afforded [cat][(L)Co(η^3-P$_3$GeAr′Cl)(CN)] (**2a**: L = PHDI, [cat]$^+$ = [*n*Bu$_4$N]$^+$; **2b**: L = Ar*BIAN, [cat]$^+$ = [K(18c-6)]$^+$). The reactivity of **2a** was studied toward group 14 electrophiles, yielding neutral germatriphosphido analogues [(PHDI)Co(η^3-P$_3$GeAr′Cl)(CNER$_3$)] (**3-ER$_3$**, ER$_3$ = CPh$_3$, Si(*i*Pr)$_3$). Furthermore, treatment of **2a** with the group 13 Lewis acid GaCl$_3$ gave [*n*Bu$_4$N][(PHDI)Co(η^3-P$_3$GeAr′Cl)(CNGaCl$_3$)] (**4-Ga**) and [(PHDI)Co(η^3-P$_2$Ge(PAr′))(CNGaCl$_3$)] (**5-Ga**), which features a remarkable P$_3$GeAr′ ligand. Compounds **1**−**5** were isolated as crystalline materials and characterized by single-crystal X-ray diffraction and multinuclear NMR spectroscopy supported by DFT calculations.

INTRODUCTION

The activation of white phosphorus, P$_4$, by transition metals has attracted much research interest over the last decades.[1−4] This led to many complexes containing polyphosphorus ligands, and their properties were widely investigated. However, complexes that contain mixed group 14/15 ligands are rather rare. This is somehow unexpected, since RE (E = group 14 element) is isolobal with P, and hence, one would expect many complexes of that type. Only recently have significant efforts been made to establish synthetic strategies that lead to a limited number of representatives (Figure 1a). For example, the complexes **A**, containing the unique *cyclo*-P$_2$E ligands (E = Ge, Sn, Pb), were synthesized by the reaction of [P≡Nb(L^1)$_3$]$^-$ (L^1 = N(Np)Ar, Np = CH$_2$*t*Bu, Ar = 3,5-Me$_2$C$_6$H$_3$) with EX$_2$ (E = group 14 element, X = Cl, SO$_3$CF$_3$).[5] Treatment of the same niobate with Me$_3$ECl (E = Si, Sn) instead formed the trimethylsilyl- and stannyl phosphinidene complexes [Me$_3$EP=Nb(L^1)$_3$].[6] The functionalization of [(MoCp)$_2$(μ-PCy$_2$)(μ-CO)$_2$]$^-$ with R$_3$ECl (R = Ph, Me; E = Ge, Sn, Pb) yielded the tetryldiphosphenyl bridged complexes **B**.[7,8] Similarly, the stannyltriphosphirene complex **C** was accessible by salt metathesis of [(η^3-P$_3$)Nb(ODipp)$_3$]$^-$ (Dipp = 2,6-*i*Pr$_2$C$_6$H$_3$) with Ph$_3$SnCl.[9]

A similar approach enables the formation of silicon-containing polyphosphorus complexes. For instance, the chlorosilylene [L^{2}SiCl] (L^2 = (*t*BuN)$_2$CPh) reacts with either [Cp‴Co(η^3-P$_3$)]$^-$ (Cp‴ = η^5-C$_5$H$_2$*t*Bu$_3$) or [Cp*Fe(η^5P$_5$)] (Cp* = η^5-C$_5$Me$_5$). This results in complex **D**, which has a

Received: June 11, 2025
Revised: July 21, 2025
Accepted: July 22, 2025
Published: July 31, 2025

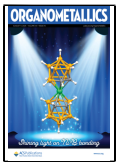

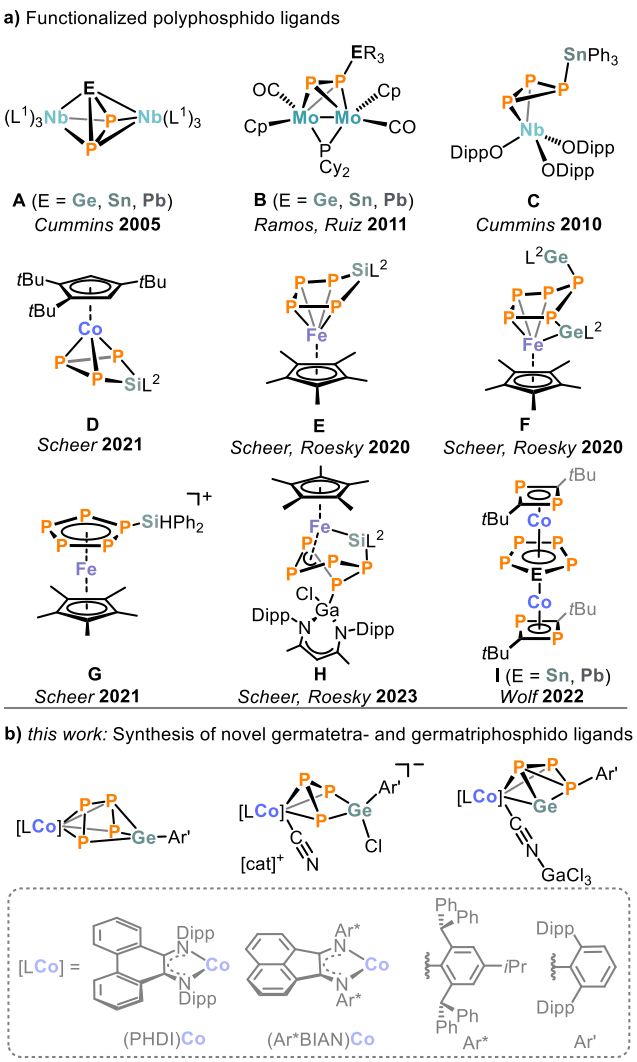

Figure 1. (a) Selected examples for functionalized polyphosphido ligands accessible via derivatization with group 14 electrophiles. (b) Synthesis of novel germatetra- and germatriphosphido ligands. L^1 = N(Np)Ar, Np = CH_2tBu, Ar = 3,5-$Me_2C_6H_3$; Cp = η^5-C_5H_5; Dipp = 2,6-iPr$_2C_6H_3$; L^2 = (tBuN)$_2$CPh; R = Ph, Me; 18c-6 = [18]-crown-6; [cat]$^+$ = [nBu$_4$N]$^+$ for L = PHDI; [cat]$^+$ = [K(18c-6)]$^+$ for L = Ar*BIAN; PHDI = bis(2,6-diisopropylphenyl)phenanthrene-9,10-diimine; BIAN = 1,2-bis(arylimino)acenaphthene; Ar* = 2,6-dibenzhydryl-4-isopropylphenyl; Ar′ = 2,6-Dipp$_2C_6H_3$.

heteroatomic *cyclo*-P_4SiL^2 ligand,[10] and the silaphosphaferrocene derivative **E**,[11] respectively. The germanium analogue [L^2GeCl] remains unreactive with [Cp*Fe(η^5-P_5)].[12] Conversely, the reaction of [Cp*Fe(η^5-P_5)] with a digermylene, [L^2Ge−GeL^2] produces the 1,2-digermylene complex **F**, derived from its 1,1-isomer.[12] Additionally, the electrophilic functionalization of [Cp*Fe(η^5P_5)] with in situ generated Ph_2SiH^+ leads to compound **G**.[13] Furthermore, a reaction with a gallasilylene yields compound **H**. There is also a report of complex **I**, which features an aromatic *cyclo*-P_4E (E = Sn, Pb) middle deck.[14]

As highlighted, the functionalization of polyphosphorus ligands with tetrylenes may result in complexes in which a group 14 element is either incorporated into a cyclic ligand framework (see Figure 1a, complexes **A**, **D**, **E**, and **I**) or acts as a substituent on a P_n ring (complexes **B**, **C**, **F**−**H**). While RSi units preferentially insert into P−P bonds, the LGe units generally act as substituents, except in complexes **A**. This might be due to the stabilizing effect of the ligand on the Si or Ge starting material, in addition to the more pronounced s character of the lone pair on Ge vs Si. We hypothesized that using bulky aryl substituents might favor incorporating the RE unit into the P_n ligand core. First evidence supporting this was provided by the reaction of [Ar′ECo(η^4-P_2C_2tBu$_2$)(η^4-COD)] (E = Sn, Pb) with P_4, which produces **I** featuring a *cyclo*-P_4E center deck.[14] In addition, we previously showed that R_2PCl reacts with [K(18c-6)][(L)Co(η^4-P_4)] (**J**, L = PHDI; **K**, L = Ar*BIAN; 18c-6 = 18-crown-6) and [cat][(PHDI)Co(CN)-(η^3-P_3)] (**L**, L = PHDI, [cat]$^+$ = [nBu$_4$N]$^+$; **M**, L = Ar*BIAN, [cat]$^+$ = [K(18c-6)]$^+$) to form polyphosphorus ligands with four to seven P atoms.[15,16] We anticipated similar reactivity of complexes **J**−**M** toward RGeCl. We now present the synthesis and characterization of the first germatetraphosphido and germatriphosphido complexes **1** and **2**, synthesized by the reaction of **J**−**M** with [Ar′GeCl]$_2$ (Ar′ = 2,6-(2,6-iPr$_2C_6H_4$)$_2$-C_6H_3). Additionally, we conducted reactivity studies of the PHDI complex **2a** with group 14 electrophiles and group 13 Lewis acids. These studies led to the isolation of isonitrile complexes **3-ER$_3$** (where ER$_3$ = CPh$_3$, Si(iPr)$_3$) and $GaCl_3$ adducts **4-Ga** and **5-Ga**. The molecular structure of **5-Ga** features a remarkable P_3Ge ligand formed through aryl migration.

RESULTS AND DISCUSSION

To synthesize mixed group 14/15 ligands, we treated compounds **J** and **K** with [Ar′GeCl]$_2$ in toluene at room temperature (see Scheme 1). After workup, we obtained dark

Scheme 1. Synthesis of [(L)Co(η^4-P_4GeAr′)] (1a,b)[a]

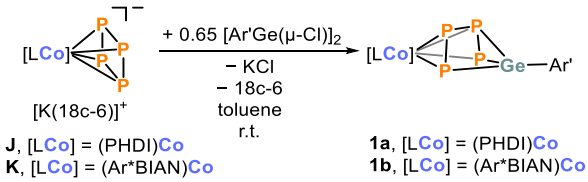

[a]Yields and conditions: for L = PHDI: 30 min, isolated yield: 36%; for L = Ar*BIAN: 1d, isolated yield: 35%.

blue crystals of [(L)Co(η^4-P_4GeAr′)] (**1a**, L = PHDI; **1b**, L = Ar*BIAN; Scheme 1), which were isolated in 36% and 35% yield for **1a** and **1b**, respectively. Single-crystal X-ray diffraction (SCXRD) analyses (see Figure 2a for **1a** and Figure S55 for **1b**) indicate that the P_4GeAr′ ligand adopts an envelope conformation, resulting from the insertion of an Ar′Ge unit into a P−P bond of **J** and **K**. Moreover, the Ge atom is connected to one distant P atom. The P_4GeAr′ ligand is coordinated through the four P atoms.

The *cyclo*-P_4GeAr′ ligand in **1a,b** is reminiscent of the sila- and gallatetraphosphacyclopentadienyl ligand in [Cp*Fe(η^4-P_4SiL^2)] (**E**, L^2 = (tBuN)$_2$CPh, Figure 1a) and [K(THF)$_2$]-[(^{Mes}BIAN)Co{η^4-P_4Ga(^{Dipp}nacnac)}] (^{Mes}BIAN = 1,2-bis-(2,4,6-dimethylphenylimino)acenaphthene, ^{Dipp}nacnac = CH-[C(Me)N(2,6-iPr$_2C_6H_3$)]$_2$), respectively.[11,17] In the slightly puckered P_4 unit of **1a**, the terminal P−P bond lengths (P1−P2: 2.145(2) Å, P3−P4: 2.1223(19) Å) are shorter than the internal P2−P3 single bond (2.2764(15) Å). The large separation between the terminal atoms P1 and P4 of 3.349(3) Å indicates minimal interaction (compared to the sum of covalent radii: Σr_{PP} 2.22 Å). The distances of P1−Ge1

https://doi.org/10.1021/acs.organomet.5c00214
Organometallics 2025, 44, 1721−1727

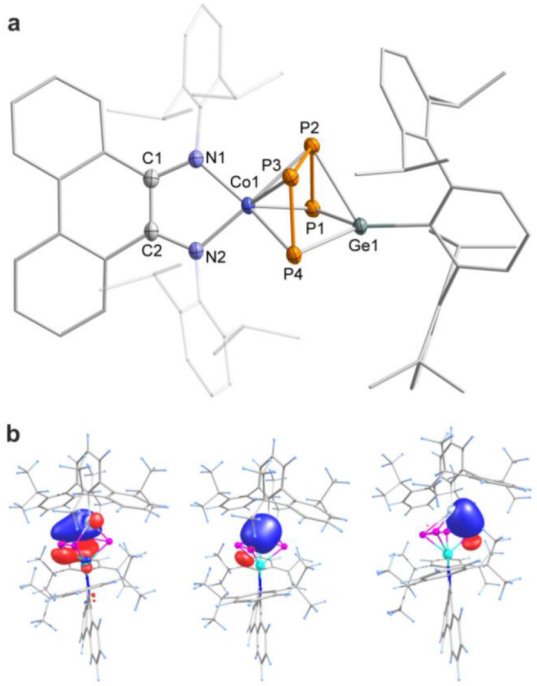

Figure 2. (a) Solid-state molecular structure of **1a**. Hydrogen atoms and solvate molecules are omitted for clarity. Thermal ellipsoids are drawn at the 50% probability level. Selected bond lengths [Å] and angles [°]: C1−C2 1.427(2), C1−N1 1.352(2), C2−N2 1.3542(19), Co1−N1 1.9171(13), Co1−N2 1.8849(13), Co1−P1 2.335(3), Co1−P2 2.3685(18), Co1−P3 2.2677(17), Co1−P4 2.3645(19), P1−P2 2.145(2), P2−P3 2.2764(15), P3−P4 2.1223(19), P1−Ge1 2.332(3), P2−Ge1 2.590(4), P3···Ge1 2.729(3), P4−Ge1 2.280(3), P1−P2−P3 105.12(14), P2−P3−P4 103.47(12). (b) Selected Intrinsic Bonding Orbitals in **1a** showing the 3c2e bond (left) and two Ge−P sigma bonds (middle and right) at the r^{2}SCAN-3c level of theory.

and P4−Ge1 (2.332(3) and 2.280(3) Å, respectively) align with the calculated value for a P−Ge single bond (Σr_{GeP} 2.32 Å) while the P2−Ge1 distance of 2.590(4) Å is slightly elongated.[18,19] Compound **1b** displays very similar metric parameters (see Supporting Information). To support the bonding scenario within the P_4Ge ligand, we optimized the structure of **1a** utilizing the composite r^{2}SCAN-3c method. The bond lengths and angles of the optimized structure closely match the experimental data. An intrinsic bond orbital (IBO) analysis (see Figure 2b and Supporting Information for details) revealed a 3-center-2-electron bond among the internal phosphorus atoms P2 and P3 and the Ge atom. In contrast, the other P−Ge bonds are identified as single bonds (Figure 2b). The Mayer Bond Order (MBO) corroborates these results, showing values of 0.40 and 0.24 for Ge1−P2 and Ge1−P3, alongside 0.75 and 0.79 for Ge1−P1 and Ge1−P4, respectively. The C−C and C−N bond lengths of the PHDI backbone suggest that it is present in its radical anionic form.[20]

The $^{31}P\{^1H\}$ NMR spectrum of the isolated crystals of **1a** recorded in toluene-d_8 shows a sharp singlet ($\Delta\nu_{1/2}$ = 15 Hz) at δ = 62.7 ppm (δ = 75.7 ppm, $\Delta\nu_{1/2}$ = 380 Hz for **1b**), rather than the expected four resonances based on the solid-state structure of **1a,b**. This indicates a dynamic process that renders all phosphorus atoms equivalent on the NMR time scale. Variable temperature (VT) $^{31}P\{^1H\}$ NMR spectroscopy (Figure S32) revealed significant signal broadening ($\Delta\nu_{1/2}$ = 272 Hz) at −80 °C but no decoalescence, indicating that the dynamic process is fast at that temperature. In contrast, in the $^{31}P\{^1H\}$ NMR spectrum of **1b** at −80 °C, four distinct, albeit broad resonances can be detected, in agreement with the solid-state structure (Figure S33). A similar dynamic behavior was reported for the stannylated *cyclo*-P_3 complex [(η^2-Ph_3SnP_3)-$Nb(ODipp)_3$].[9]

Next, the reactivity of the *cyclo*-P_3 complexes **K** and **L** toward [Ar′GeCl]$_2$ (0.5 equiv) was investigated. After workup, dark purple crystals of **2a,b** were obtained in yields of 49% (**2a**) and 65% (**2b**), respectively (Scheme 2). SCXRD analyses

Scheme 2. Synthesis of [cat][(L)Co(η^3-P_3GeAr′Cl)(CN)] (2a,b)[a]

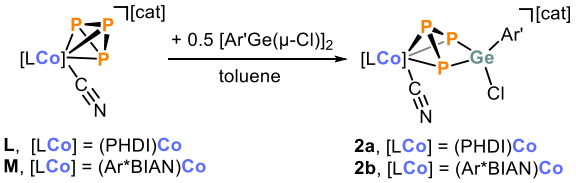

[a]Conditions for L = PHDI: [cat]$^+$ = [nBu$_4$N]$^+$; 40 °C, 1 d, isolated yield: 49%; for L = Ar*BIAN: [cat]$^+$ = [K(18c-6)]$^+$; r.t., 4 d, isolated yield: 65%.

revealed the formation of [cat][(L)Co(η^3-P_3GeAr′Cl)(CN)] (**2a**, L = PHDI, [cat]$^+$ = [nBu$_4$N]$^+$, Figure 3; **2b**, L = Ar*BIAN, [cat]$^+$ = [K(18c6)]$^+$, Figure S56), generated via the insertion of a Ar′GeCl moiety into one P−P bond of the *cyclo*-P_3 ring.

Complex **2a** crystallizes as separated ion pairs (Figure 3a), whereas in **2b**, the [K(18c-6)]$^+$ cation is coordinated to the N atom of the cyanide ligand (Figure S56). The anions show a puckered *cyclo*-P_3GeAr′Cl ligand that coordinates η^3 to the cobalt atom. The P−P bond lengths (**2a**: P1−P2 2.1678(15), P1−P3 2.1817(14) Å; **2b**: P1−P2 2.1787(6), P1−P3 2.1882(6) Å) are situated between a P−P single bond (Σr_{PP} 2.22 Å) and a P=P double bond (Σr_{PP} 2.04 Å), suggesting delocalized multiple bond character. In contrast, the P−Ge bond lengths (**2a**: P2−Ge1 2.2968(11), P3−Ge1 2.2924(10) Å; **2b**: P2−Ge1 2.2996(5), P3−Ge1 2.3114(5) Å) are consistent with the calculated value for a P−Ge single bond derived from the sum of covalent radii (Σr_{GeP} 2.32 Å).[18,19] The long P2−P3 distances of 3.093(1) Å (**2a**) and 3.098(6) Å (**2b**) indicate no interaction between these atoms. The coordination sphere of cobalt is completed by either the formally radical anionic PHDI (**2a**) or Ar*BIAN (**2b**) ligands, along with a CN^- ligand.[20] The IR spectra show strong absorption bands at $\tilde{\nu}_{CN}$ = 2088 cm^{-1} (**2a**) and 2076 cm^{-1} (**2b**), attributed to the CN^- ligand.

To the best of our knowledge, the insertion of a low-coordinate germanium center into a P−P bond has only been noted in the reaction of a diarylgermylene or an electron-rich germylene toward white phosphorus.[21,22] The closest related complex to **2a,b** is [Cp‴Co(η^3-P_3SiL^2)] (**D**, Cp‴ = $C_5H_2tBu_3$, L^2 = (tBuN)$_2$CPh, Figure 1a), while similar complexes featuring *cyclo*-P_3Ge ligands appear to be unreported.[10] Germanium-containing (poly)phosphorus ligands have been documented in the complexes **A**, **B**, and **F** (Figure 1a).[5,7,12]

The $^{31}P\{^1H\}$ NMR spectrum of isolated **2a** in C_6D_6 at room temperature features an A_2M spin system at δ = 179.4 ppm (P_A) and δ = 1.9 ppm (P_M) (Figure 3b; cf. compound **2b**: δ = 160.6 (P_A), −30.6 ppm (P_X); Figure S15). In addition, low-intensity signals of an A_2M spin system can be detected, which

https://doi.org/10.1021/acs.organomet.5c00214
Organometallics 2025, 44, 1721−1727

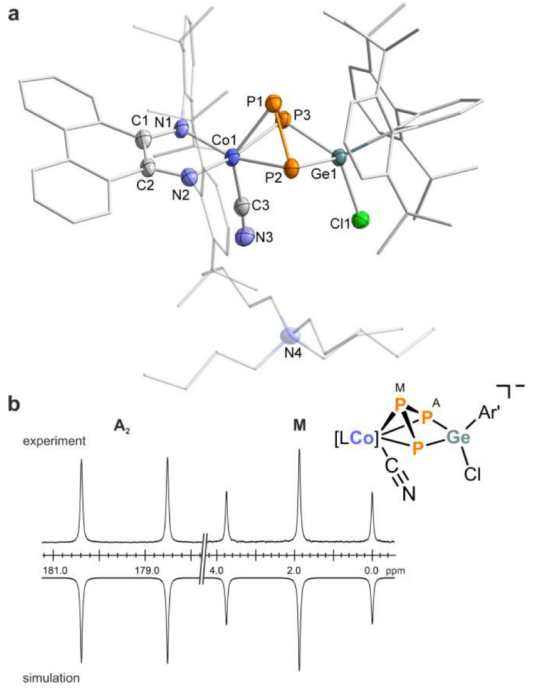

Figure 3. (a) Solid-state molecular structure of **2a**. Hydrogen atoms and solvate molecules are omitted for clarity. Thermal ellipsoids are drawn at the 50% probability level. Selected bond lengths [Å] and angles [°]: C1−C2 1.432(6), C1−N1 1.348(5), C2−N2 1.342(5), Co1−C3 1.916(4), Co1−N1 1.922(3), Co1−N2 1.949(3), Co1−P1 2.2601(12), Co1−P2 2.3495(12), Co1−P3 2.3280(11), C3−N3 1.158(5), P1−P2 2.1678(15), P1−P3 2.1817(14), P2−P3 3.093(1), P2−Ge1 2.2968(11), P3−Ge1 2.2924(10), Ge1−Cl1 2.2398(10)*, P2−P1−P3 90.65(5), Ge1−P2−P1 79.32(4), Ge1−P3−P1 79.71(4), P3−Ge1−P2 84.75(4); *bond length results from the disordered part with the highest occupancy; [LCo] = (PHDI)Co. (b) Section of the $^{31}P\{^{1}H\}$ NMR spectrum of compound **2a** with nuclei assigned to an A_2M spin system; experimental (upward); simulation (downward): $\delta(P_A)$ = 179.4 ppm, $\delta(P_M)$ = 1.89 ppm; $^{1}J_{AM}$ = −304.0 Hz.

are tentatively attributed to the iodo derivative of **2a,b**, based on the calculated ^{31}P NMR chemical shifts (see Tables S15–17). The iodine atom likely originates from trace impurities in the starting material $[Ar'GeCl]_2$, which was synthesized from Ar′I (see Figure S10 and the crystallographic chapter in the SI). Nevertheless, C, H, N combustion analyses agree well with the compositions of **2a,b**.

We also examined the reactivity of **L** and **M** with $[Ar'Sn(\mu\text{-}Cl)]_2$. Based on $^{31}P\{^{1}H\}$ NMR spectroscopic studies, the Ar′SnCl unit fails to insert into the P−P bond, as no signals indicative of an A_2M spin system corresponding to the tin derivative of **2a,b** were detected (for additional details, see the Supporting Information). $[Ar'Pb(\mu\text{-}Br)]_2$ shows no reaction with **L** or **M**.

Intending to synthesize neutral isocyanido analogues, we treated **2a** with one equivalent of group 14 triflates R_3EOTf (R_3E = Ph_3C, iPr_3Si, Me_3Si; Scheme 3). The reactions proceed selectively at room temperature as shown by $^{31}P\{^{1}H\}$ NMR spectroscopy. SCXRD analysis on two of the reaction products, **3-CPh$_3$** and **3-Si(*i*Pr)$_3$**, revealed the formation of $[(PHDI)Co(\eta^3\text{-}P_3GeAr'Cl)(CNER_3)]$ (**3-ER$_3$**, Figures S58 and S59), i.e., the bonding of the nitrogen atom of the CN ligand in **2a** to the electrophile.

Intending to remove the chloride attached to Ge, we treated **2a** with the stronger Lewis acids ECl_3 (E = Ga, Al).[23−25] The

Scheme 3. Synthesis of Compounds 3-ER$_3$[a]

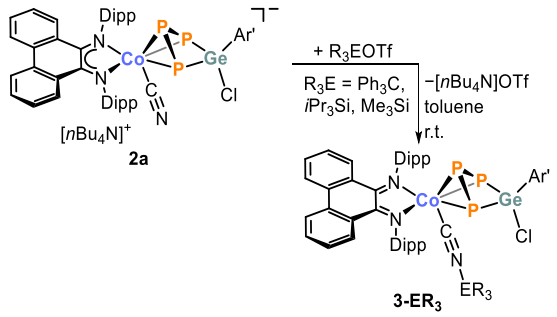

[a]Conditions: 16 h for R_3E = CPh_3, 23 h for R_3E = iPr_3Si; isolated yields **3-CPh$_3$**: 44%, **3-Si(*i*Pr)$_3$**: 65%.

reaction of **2a** with one equivalent of $GaCl_3$ led to the formation of the Lewis acid adduct $[nBu_4N][(PHDI)Co(\eta^3\text{-}P_3GeAr'Cl)(CNGaCl_3)]$ (**4-Ga**, Scheme 4).

Scheme 4. Synthesis of $[nBu_4N][(PHDI)Co(\eta^3\text{-}P_3GeAr'Cl)(CNGaCl_3)]$ (4-Ga)[a]

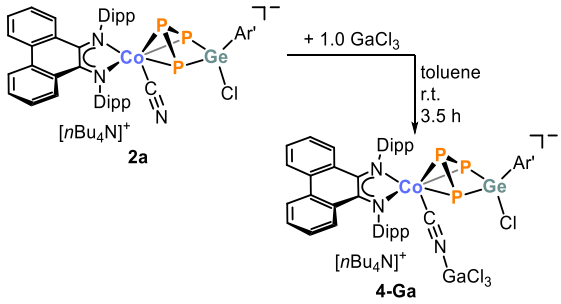

[a]Isolated yield 64%.

The $^{31}P\{^{1}H\}$ NMR spectrum of isolated **4-Ga** in C_6D_6 closely resembles that of **3-ER$_3$**, exhibiting an A_2M spin system with resonances at δ = 173.1 ppm (P_A) and δ = 30.4 ppm (P_M). The ^{31}P NMR chemical shifts calculated by DFT at the r^{2}SCAN-3c level of theory (177 and 66 ppm) agree well with the experimental ones, supporting the structural proposal (Table S15). A second A_2M spin system [δ = 168.6 ppm (P_A), δ = 18.6 ppm (P_M)] with low intensity (15%) in the $^{31}P\{^{1}H\}$ NMR spectrum of **4-Ga** suggests the presence of a second species in solution (Figure S26), which could be attributed to a configurational isomer or the iodo derivative of **4-Ga**. All attempts to grow X-ray quality single crystals of **4-Ga** resulted only in weakly diffracting dark blue crystals, which prevented the collection of a reasonably good data set. Nonetheless, multinuclear NMR spectroscopy and C, H, N combustion analysis on the isolated compound support the molecular composition of compound **4-Ga**.

When **2a** reacts with two equivalents of ECl_3 (where E = Ga or Al) at 40 °C in toluene, a new compound is formed selectively over 8 days, resulting in an AMX spin system observed in the $^{31}P\{^{1}H\}$ NMR spectrum (Scheme 5). Dark blue crystals of **5-Ga** were isolated from toluene/*n*-hexane in 21% isolated yield. Unfortunately, **5-Al** has eluded all efforts of isolation as a pure compound; however, in one case, a single crystal could be picked. SCXRD experiments confirmed the formation of $[(PHDI)Co(\eta^3\text{-}P_2Ge(PAr'))(CNECl_3)]$ (**5-E**, Figure 4 for E = Ga and Figure S60 for E = Al).

https://doi.org/10.1021/acs.organomet.5c00214
Organometallics 2025, 44, 1721−1727

Scheme 5. Synthesis of [(PHDI)Co(η^3-$P_2Ge(PAr')$)($CNGaCl_3$)] (5-Ga)[a]

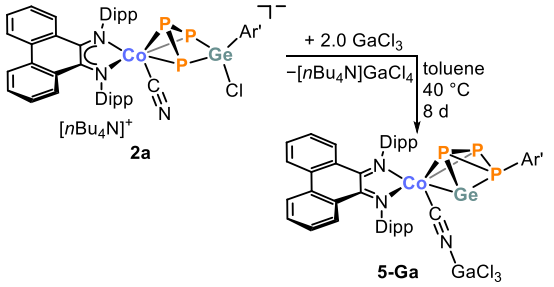

[a]Isolated yield: 21%

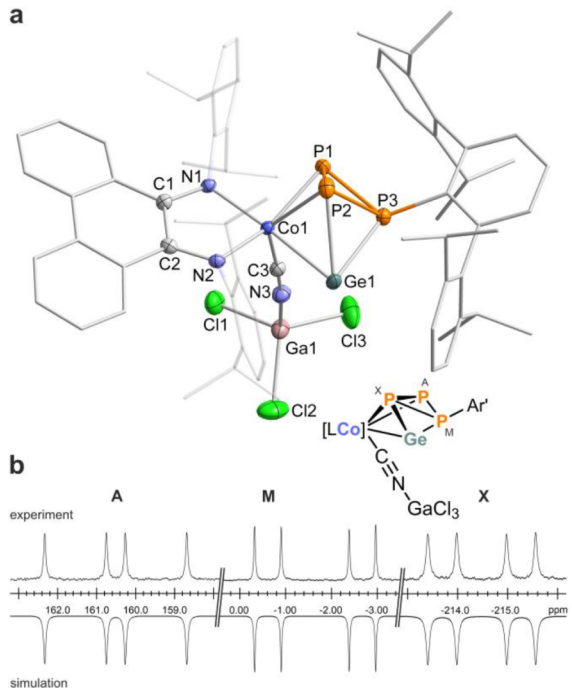

Figure 4. (a) Solid-state molecular structure of **5-Ga**. Hydrogen atoms and solvate molecules are omitted for clarity. Thermal ellipsoids are drawn at the 50% probability level. The P_3GeAr' fragment showed site disorder. Bond lengths [Å] and angles [°] of the major part: C1−C2 1.461(2), C1−N1 1.328(2), C2−N2 1.329(2), Co1−C3 1.8621(18), Co1−N1 1.9546(14), Co1−N2 1.9450(15), Co1−P1 2.2589(12), Co1−P2 2.3501(17), Co1−Ge1 2.4413(4), C3−N3 1.165(2), N3−Ga1 1.9303(16), P1−P2 2.1473(16), P1−P3 2.1316(12), P2−P3 2.2732(17), P2−Ge1 2.5070(14), P3−Ge1 2.3969(5), P2−P1−P3 64.18(5), P1−P3−P2 58.25(5), P1−P2−P3 57.58(5), Ge1−P2−P3 59.95(4), Ge1−P3−P2 64.87(4), P3−Ge1−P2 55.18(4), P1−Co1−Ge1 93.52(3), Co1−Ge1−P3 78.646(15), Ge1−P3−P1 98.16(3), P3−P1−Co1 88.54(4). (b) Section of the $^{31}P\{^1H\}$ NMR spectrum of **5-Ga** with nuclei assigned to an AMX spin system; experimental (upward); simulation (downward): $\delta(P_A)$ = 160.5 ppm, $\delta(P_M)$ = −1.6 ppm, $\delta(P_X)$ = −214.5 ppm; $^1J_{AM}$ = −334.5 Hz, $^1J_{MX}$ = −94.0 Hz, $^1J_{AX}$ = −255.7 Hz; [LCo] = (PHDI)Co.

The salient feature of **5-E** is the unusual $P_2Ge(PAr')$ ligand coordinating to the cobalt atom in an η^3-mode through the atoms P1, P2 and Ge1 (Figure 4). Thus, upon removal of the chloride, the P_3Ge core rearranges, accompanied by the migration of the terphenyl substituent from Ge to P. According to the bond lengths, the PHDI ligand is present in its neutral form.[26−28] An isocyanido ligand completes the coordination sphere of cobalt. For the latter, a strong absorption band at $\tilde{\nu}_{CN}$ = 2061 cm^{-1}, attributed to the CN stretch, is detected in the IR spectrum of isolated **5-Ga**.

In **5-Ga**, the CoP_3Ge core represents a slightly distorted square pyramid, with P1, Co1, Ge1 and P3 forming the square base and P2 representing the pyramid's apex (distance to the square center 1.655(1) Å). The Co1−Ge1−P3 angle (78.646(15)°) within the square base is more acute compared to the other angles, due to the longer Ge−Co and Ge−P bond lengths (P3−Ge1 2.3969(5) Å, Co1−Ge1 2.4413(4) Å vs. P1−P3 2.1316(12) Å, Co1−P1 2.2589(12) Å). The P1−P2 (2.1473(16) Å) and P1−P3 (2.1316(12) Å) bond lengths lie between the values calculated for P−P single (Σr_{PP} 2.22 Å) and P=P double (Σr_{PP} 2.04 Å) bonds, while the P2−P3 distance is slightly greater (2.2732(17) Å). The P−Ge distances (av. 2.4520 Å) are longer than a P−Ge single bond (Σr_{GeP} 2.32 Å) but are comparable to those reported for the *cyclo*-GeP_2 ligand (av. 2.4465 Å) in **A** (Figure 1a, vide supra).[5,18] DFT calculations for **5-Ga** at the r^{2}SCAN-3c level of theory support the description of the Co−P, P−P and P−Ge bonds as single bonds (see Supporting Information).

The compounds [{(^{Dipp}nacnac)Ga(Cl)P}(P_3GeAr^{Me6})] (Ar^{Me6} = 2,6-$Mes_2C_6H_3$),[22] [(μ,$\eta^{3:3}$-*cyclo*-GeP_2){Nb[N(Np)-Ar]$_3$}$_2$] (**A**, see Figure 1 above), and [{Nb(ODipp$_3$)η^3-P_3}$_2$(μ-Sn)] are related to **5-Ga**, featuring mixed germanium- and tin-containing polyphosphido ligands.[9,29] To the best of our knowledge, no other examples of germanium incorporation in polyphosphorus ligands are reported.

The $^{31}P\{^1H\}$ NMR spectrum of **5-Ga** recorded in CD_2Cl_2 at room temperature displays three resonances exhibiting an AMX spin system at $\delta(P_A)$ = 160.5 ppm, $\delta(P_M)$ = −1.6 ppm and $\delta(P_X)$ = −214.5 ppm. The DFT-calculated chemical shifts corroborate this assignment (see Table S16). The $^{31}P\{^1H\}$ NMR spectrum was successfully simulated using an iterative fitting procedure (Figures 4 and S31). The resulting data revealed one small $^1J_{PMPX}$ (−94.0 Hz) and two large $^1J_{PP}$ (−334.5, −255.7 Hz) couplings (Figure 4). The resonances assigned to P_A and P_X are slightly broadened, likely due to interactions with the quadrupolar ^{59}Co nucleus.

To gain further insight into the formation of **5-E**, we monitored the reaction progress by heteronuclear NMR spectroscopy (see Figures 5 and S38 for the reaction of **2a** with $GaCl_3$; Figure S39 for the reaction with $AlCl_3$, SI). Scheme 6 illustrates the proposed reaction mechanism derived from these findings. The reaction of **2a** with ECl_3 in CD_2Cl_2 at room temperature initially forms **4-E** through cyanide coordination with the Lewis acid (Scheme 6a). This is supported by the successful isolation of **4-Ga** (as mentioned above) and the characteristic A_2M spin system ($\delta(P_A)$ = 172.0 ppm, $\delta(P_M)$ = 28.9 ppm) observed in the $^{31}P\{^1H\}$ NMR spectrum for the $AlCl_3$ derivative **4-Al** (Figure S39). Addition of another equivalent of Lewis acid converts **4-E** into a new compound exhibiting an A_2X spin system [E = Ga: δ = 335.1 (P_A), δ = −158.5 ppm (P_X), Figure 5b; E = Al: δ = 334.4 (P_A), δ = −161.9 ppm (P_X), Figure S39] in the $^{31}P\{^1H\}$ NMR spectrum. After stirring at room temperature for 4 days, additional signals corresponding to an AMX spin system appear, characteristic of **5-E**, indicating the rearrangement of the P_3Ge core and the migration of the Ar′ substituent from germanium to phosphorus (Figures 5c and S39). This transformation accelerates at a slightly higher temperature (33 °C; Figure 5d). In all attempts to crystallize **Int-E**, only single crystals of **5-Ga** were obtained, likely due to the

https://doi.org/10.1021/acs.organomet.5c00214
Organometallics 2025, 44, 1721−1727

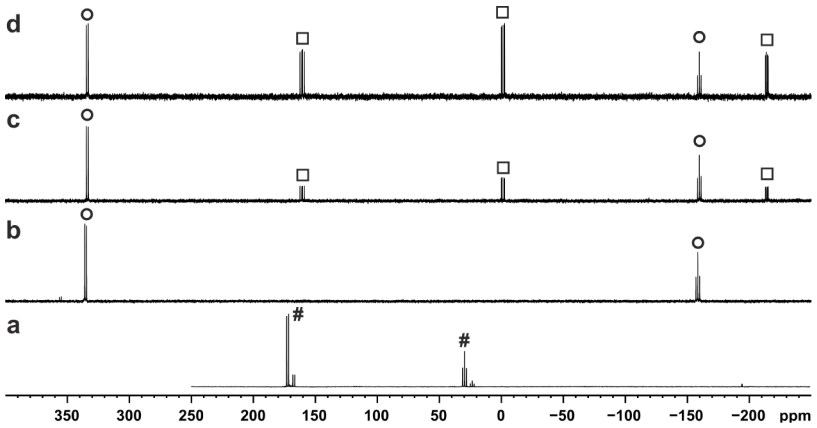

Figure 5. $^{31}P\{^{1}H\}$ NMR spectra (162.04 MHz, 300 K, CD_2Cl_2) of the reaction between $[nBu_4N][(PHDI)Co(CN)(\eta^3\text{-}P_3GeAr'Cl)]$ (**2a**) and (a) one equivalent $GaCl_3$; (b) two equivalents $GaCl_3$ after 3 h at r.t.; (c) two equivalents $GaCl_3$ after 4 days at r.t. and (d) two equivalents $GaCl_3$ after 2 days at 33 °C. # = **4-Ga**; ○ = **Int-Ga**, □ = **5-Ga**.

Scheme 6. Proposed Mechanism of Formation of Compounds 5-E

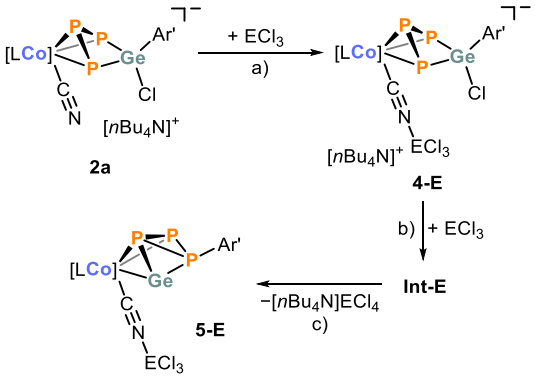

significant difference in solubility between **Int-E** and **5-E**. The formation of **4-Ga** was not observed when **2a** was treated with two equivalents of $GaCl_3$. Instead, the $^{31}P\{^{1}H\}$ NMR spectrum displayed characteristic signals for **Int-Ga** and **5-Ga**.

CONCLUSION

This study presents the synthesis and characterization of polyphosphido complexes featuring mixed germanium−phosphorus ligands. The neutral complexes **1a,b** and the anionic complexes **2a,b** are formed by insertion of an Ar′GeCl unit into a P−P bond within the *cyclo*-P_4 and *cyclo*-P_3 complexes **J**, **K**, **L**, and **M**, respectively. Salt metathesis of **2a** with group 14 triflates R_3EOTf (R_3E = Ph_3C, iPr_3Si) produces the neutral isocyanido complexes **3-ER$_3$**. Furthermore, the reaction of **2a** with strong Lewis acids $GaCl_3$ and $AlCl_3$ leads to chloride abstraction and a rearrangement of the P_3Ge ligand, yielding complexes **5-E** (E = Al, Ga) that have an unusual $CoP_2Ge(PAr')$ core. NMR spectroscopic studies validate the formation mechanism for **5-E** through two intermediates: the isolable anionic Lewis acid adduct **4-Ga** and the subsequent intermediate **Int-E**, which is generated from the elimination of $[nBu_4N][ECl_4]$. This research underscores the potential of polyphosphido complexes for selective functionalization using group 14 halides and provides valuable insights into reactivity patterns and mechanisms through the successful generation of rare, mixed group 14/15 ligands.

ASSOCIATED CONTENT

Supporting Information

The Supporting Information is available free of charge at https://pubs.acs.org/doi/10.1021/acs.organomet.5c00214.

All synthetic procedures, NMR, UV/vis, and IR spectroscopic data of compounds **1**−**5**, additional experiments, crystallographic data of compounds **1**−**5**, and computational details (PDF)

Cartesian coordinates of all calculated structures (XYZ)

Accession Codes

Deposition numbers 2448599, 2448601, and 2448607−2448612 contain the supplementary crystallographic data for this paper. These data can be obtained free of charge via the joint Cambridge Crystallographic Data Centre (CCDC) and Fachinformationszentrum Karlsruhe Access Structures service.

AUTHOR INFORMATION

Corresponding Author

Robert Wolf − *Institute of Inorganic Chemistry, University of Regensburg, Regensburg 93040, Germany*; orcid.org/0000-0003-4066-6483; Email: robert.wolf@ur.de

Authors

Karolina Trabitsch − *Institute of Inorganic Chemistry, University of Regensburg, Regensburg 93040, Germany*

Sebastian Hauer − *Institute of Inorganic Chemistry, University of Regensburg, Regensburg 93040, Germany*; orcid.org/0009-0009-9963-4751

Gábor Balázs − *Institute of Inorganic Chemistry, University of Regensburg, Regensburg 93040, Germany*

Jan J. Weigand − *Faculty of Chemistry and Food Chemistry, Technische Universität Dresden, Dresden 01062, Germany*; orcid.org/0000-0001-7323-7816

Complete contact information is available at: https://pubs.acs.org/10.1021/acs.organomet.5c00214

Author Contributions

The manuscript was written through contributions of all authors. All authors have given approval to the final version of the manuscript.

Notes

The authors declare no competing financial interest.

■ ACKNOWLEDGMENTS

We thank Lukas Dopfer and Lukas Schober for experimental assistance. Generous financial support of this work by the Deutsche Forschungsgemeinschaft (DFG, projects WE4621/3-2, WO1496/7-2, and WO1496/10-2) is gratefully acknowledged.

■ REFERENCES

(1) Cossairt, B. M.; Piro, N. A.; Cummins, C. C. Early-Transition-Metal-Mediated Activation and Transformation of White Phosphorus. *Chem. Rev.* **2010**, *110*, 4164−4177.
(2) Caporali, M.; Gonsalvi, L.; Rossin, A.; Peruzzini, M. P_4 Activation by Late-Transition Metal Complexes. *Chem. Rev.* **2010**, *110* (7), 4178−4235.
(3) Hoidn, C. M.; Scott, D. J.; Wolf, R. Transition-Metal-Mediated Functionalization of White Phosphorus. *Chem. − Eur. J.* **2021**, *27* (6), 1886−1902.
(4) Giusti, L.; Landaeta, V. R.; Vanni, M.; Kelly, J. A.; Wolf, R.; Caporali, M. Coordination Chemistry of Elemental Phosphorus. *Coord. Chem. Rev.* **2021**, *441*, 213927.
(5) Figueroa, J. S.; Cummins, C. C. Triatomic EP_2 Triangles (E = Ge, Sn, Pb) as μ^2:η^3,η^3-Bridging Ligands. *Angew. Chem., Int. Ed.* **2005**, *44*, 4592−4596.
(6) Figueroa, J. S.; Cummins, C. C. Diorganophosphanylphosphinidenes as Complexed Ligands: Synthesis via an Anionic Terminal Phosphide of Niobium. *Angew. Chem., Int. Ed.* **2004**, *43*, 984−988.
(7) Alvarez, M. A.; García, M. E.; García-Vivó, D.; Ramos, A.; Ruiz, M. A. Mild P_4 Activation To Give an Anionic Diphosphorus Complex with a Dual Binding Ability at a Single P Site. *Inorg. Chem.* **2011**, *50*, 2064−2066.
(8) Alvarez, M. A.; García, M. E.; García-Vivó, D.; Ramos, A.; Ruiz, M. A. Reactivity of the Anionic Diphosphorus Complex $[Mo_2Cp_2(\mu\text{-}PCy_2)(CO)_2(\mu\text{-}\kappa^2\text{:}\kappa^2\text{-}P_2)]^-$ Toward ER_3X Electrophiles (E = C to Pb): Insights into the Multisite Donor Ability and Dynamics of the P_2 Ligand. *Inorg. Chem.* **2012**, *51*, 11061−11075.
(9) Cossairt, B. M.; Cummins, C. C. Shuttling P_3 from Niobium to Rhodium: The Synthesis and Use of $Ph_3SnP_3(C_6H_8)$ as a P_3^- Synthon. *Angew. Chem., Int. Ed.* **2010**, *49*, 1595−1598.
(10) Piesch, M.; Reichl, S.; Seidl, M.; Balázs, G.; Scheer, M. Synthesis and Multiple Subsequent Reactivity of Anionic *cyclo*-E_3 Ligand Complexes (E = P, As). *Angew. Chem., Int. Ed.* **2021**, *60*, 15101−15108.
(11) Yadav, R.; Simler, T.; Reichl, S.; Goswami, B.; Schoo, C.; Köppe, R.; Scheer, M.; Roesky, P. W. Highly Selective Substitution and Insertion Reactions of Silylenes in a Metal-Coordinated Polyphosphide. *J. Am. Chem. Soc.* **2020**, *142*, 1190−1195.
(12) Yadav, R.; Goswami, B.; Simler, T.; Schoo, C.; Reichl, S.; Scheer, M.; Roesky, P. W. A Bis(Germylene) Functionalized Metal-Coordinated Polyphosphide and Its Isomerization. *Chem. Commun.* **2020**, *56*, 10207−10210.
(13) Riesinger, C.; Balázs, G.; Seidl, M.; Scheer, M. Substituted Aromatic Pentaphosphole Ligands − a Journey across the p-Block. *Chem. Sci.* **2021**, *12*, 13037−13044.
(14) Kelly, J. A.; Streitferdt, V.; Dimitrova, M.; Westermair, F. F.; Gschwind, R. M.; Berger, R. J. F.; Wolf, R. Transition-Metal-Stabilized Heavy Tetraphospholide Anions. *J. Am. Chem. Soc.* **2022**, *144*, 20434−20441.
(15) Hoidn, C. M.; Trabitsch, K.; Schwedtmann, K.; Taube, C.; Weigand, J. J.; Wolf, R. Formation of a Hexaphosphido Cobalt Complex through P−P Condensation. *Chem. − Eur. J.* **2023**, *29* (56), No. e202301930.
(16) Trabitsch, K.; Hauer, S.; Schwedtmann, K.; Royla, P.; Weigand, J. J.; Wolf, R. Phosphorus Ring Expansion at Cobalt: Targeted Synthesis of P_4, P_5, and P_7 Ligands. *Inorg. Chem. Front.* **2025**, *12*, 2013−2023.
(17) Ziegler, C. G. P.; Maier, T. M.; Pelties, S.; Taube, C.; Hennersdorf, F.; Ehlers, A. W.; Weigand, J. J.; Wolf, R. Construction of Alkyl-Substituted Pentaphosphido Ligands in the Coordination Sphere of Cobalt. *Chem. Sci.* **2019**, *10*, 1302−1308.
(18) Pyykkö, P.; Atsumi, M. Molecular Single-Bond Covalent Radii for Elements 1−118. *Chem. − Eur. J.* **2009**, *15*, 186−197.
(19) Pyykkö, P.; Atsumi, M. Molecular Double-Bond Covalent Radii for Elements Li−E112. *Chem. − Eur. J* **2009**, *15* (46), 12770−12779.
(20) Gao, B.; Luo, X.; Gao, W.; Huang, L.; Gao, S.; Liu, X.; Wu, Q.; Mu, Y. Chromium Complexes Supported by Phenanthrene-Imine Derivative Ligands: Synthesis, Characterization and Catalysis on Isoprene Cis-1,4 Polymerization. *Dalton Trans.* **2012**, *41*, 2755−2763.
(21) Dube, J. W.; Graham, C. M. E.; Macdonald, C. L. B.; Brown, Z. D.; Power, P. P.; Ragogna, P. J. Reversible, Photoinduced Activation of P_4 by Low-Coordinate Main Group Compounds. *Chem. − Eur. J.* **2014**, *20* (22), 6739−6744.
(22) Bücker, A.; Gehlhaar, A.; Wölper, C.; Schulz, S. Activation of Non-Polar Bonds by an Electron-Rich Gallagermylene. *Chem. Commun.* **2024**, *60*, 2902−2905.
(23) Schwedtmann, K.; Holthausen, M. H.; Sala, C. H.; Hennersdorf, F.; Fröhlich, R.; Weigand, J. J. $[(^{Cl}Im^{Dipp})PP(Dipp)][GaCl_4]$: A Polarized, Cationic Diphosphene. *Chem. Commun.* **2016**, *52*, 1409−1412.
(24) Beil, A.; Gilliard, R. J.; Grützmacher, H. From the Parent Phosphinidene−Carbene Adduct NHCPH to Cationic P_4-Rings and P_2-Cycloaddition Products. *Dalton Trans.* **2016**, *45*, 2044−2052.
(25) Villinger, A.; Westenkirchner, A.; Wustrack, R.; Schulz, A. $GaCl_3$-Assisted Cyclization Reactions in Hypersilyl(Trimethylsilyl)-Aminodichlorophosphine. *Inorg. Chem.* **2008**, *47*, 9140−9142.
(26) van Belzen, R.; Klein, R. A.; Kooijman, H.; Veldman, N.; Spek, A. L.; Elsevier, C. J. Stoichiometric and Catalytic Conversion of Alkynes to Conjugated (*Z*,*Z*)-Dienes and Cyclopentadienes via Palladacyclopentadienes and 1,3-Dienylpalladium(II) Halide and Triorganopalladium(IV) Halide Compounds Containing Chelating Nitrogen Ligands. *Organometallics* **1998**, *17*, 1812−1825.
(27) Kramer, W. W.; Cameron, L. A.; Zarkesh, R. A.; Ziller, J. W.; Heyduk, A. F. Donor−Acceptor Ligand-to-Ligand Charge-Transfer Coordination Complexes of Nickel(II). *Inorg. Chem.* **2014**, *53*, 8825−8837.
(28) Abakumov, G. A.; Druzhkov, N. O.; Kocherova, T. N.; Kozhanov, K. A.; Murugova, A. V.; Egorova, E. N. Coordination Ability of N,N'-Disubstituted 9,10-Phenanthrenediimines. *Dokl. Chem.* **2016**, *467*, 109−112.
(29) Velian, A.; Cossairt, B. M.; Cummins, C. C. Assembly and Stabilization of $\{E(cyclo\text{-}P_3)_2\}$ (E = Sn, Pb) as a Bridging Ligand Spanning Two Triaryloxyniobium Units. *Dalton Trans.* **2016**, *45*, 1891−1895.

https://doi.org/10.1021/acs.organomet.5c00214
Organometallics 2025, 44, 1721−1727